Journal of Materials Chemistry A

Accepted Manuscript

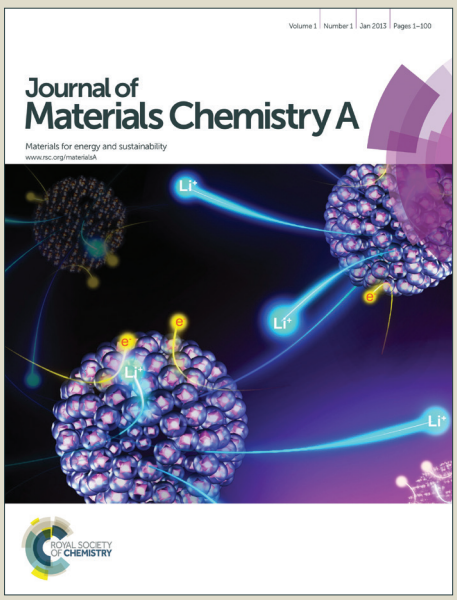

ROYAL SOCIETY OF CHEMISTRY

www.rsc.org/materialsA

Journal Name

RSCPublishing

ARTICLE

Amine-Functionalized Siloxane Oligomer Facilitated Synthesis of Subnanometer Colloidal Au Particles

Cite this: DOI: 10.1039/x0xx00000x

Zhen Wang,[a,b] Evgeny V. Beletskiy,[a] Sungsik Lee,[c] Xianliang Hou[a,b] Yuyang Wu,[d] Tiehu Li,[b] Mayfair C. Kung,[a]* and Harold H. Kung.[a]*

Received 00th January 2012,
Accepted 00th January 2012

DOI: 10.1039/x0xx00000x

www.rsc.org/

Amine-functionalized siloxane oligomers were synthesized and used successfully to prepare colloidal Au particles smaller than 1 nm. Using NMR to follow the interaction of Au(THT)Cl with the functionalized siloxane, it was determined that the amine ligands displaced the THT ligand effectively. By comparison with other functionalized siloxane oligomers/compound, parameters such as density of ligating groups, oligomer steric barrier and reduction rates were found to be essential for the formation and stability of subnanometer Au particles. Without further treatment, the formed Au particles were active catalysts for the reduction of *p*-nitrobenzaldehyde by triethylsilane, forming an imine as the major coupling product. Deposition of the Au colloids onto silica, followed by thermal treatment to remove the organic groups resulted in subnanometer Au on silica, indicating this to be a promising method of fabricating subnanometer supported Au catalyst.

A Introduction

Colloidal gold particles with diameters smaller than around 2 nm exhibit many interesting properties. When the size of a Au cluster is comparable to the Fermi wavelength, the plasmon resonance greatly diminishes, while size-dependent fluorescence and molecule-like HOMO-LUMO transition emerges.[1-7] Strong size-dependent catalytic properties have been observed in this size range.[8-12] For example, large Au particles are significantly less active in catalytic oxidation than small particles[11, 13] and in water-gas shift than atomic Au (or Au cations),[14] and there is a change in selectivity from hydrogenation to epoxidation in the reaction of propene in a mixture of H_2 and O_2 in the range of 1 to 3 nm.[9] Small Au particles have also found applications in DNA or drug delivery, as the efficiency in cell membrane penetration increases with decreasing Au particle size.[15-17] In view of these, there have been intensive effort to develop methods to synthesize small Au particles[18], particularly those 2 nm and smaller.

Among the methods explored, colloidal preparation is attractive because it is easily scalable for commercial applications. In colloidal preparation, a Au salt precursor in solution is reduced in the presence of a stabilizer. The choice of stabilizer is essential, since large Au particles would form if the stabilizer interacts too weakly with Au, whereas stabilizers that interact too strongly could alter the properties of the Au particles significantly. The propensity of Au to adsorb sulfur compounds makes thiols popular stabilizers for the preparation of small Au colloidal particles, and clusters with 1-4 nm average diameter can be prepared regularly.[19-23] In addition to thiols and phosphines,[24, 25] bifunctional stabilizers have been successfully employed also, and these include hydroxy mercapto glycol,[26] hydroxy thiolate,[27] tetraalkylammonium bromide,[28] mercaptosuccinic acid,[29] phosphonated mercapto compounds,[30] aminophosphonate,[31] and ethylenediamine tetraacetate.[32] In these bifunctional stabilizers, one functional group ligates the Au particle, and the other renders a charged layer around the particle, thereby stabilizing the particles from agglomeration by charge-charge repulsion. Recently, preparations of atomically monodisperse thiolate-stabilized clusters have been reported for Au_{11}, Au_{25}, Au_{38}, Au_{102}, Au_{144}, etc.[3, 33-36] A rapid small-scale synthetic method that produces thiolate-coated gold nanoclusters (d < 2 nm) in 2 min has also been reported.[37]

While effective in stabilizing nanosize Au particles, the strong chemical interaction of sulfur or phosphorus with Au could affect the chemical properties of the colloidal Au, especially those that depend on surface Au atoms. Removal of the stabilizer typically entails first the deposition of Au clusters on a support followed by oxidative thermal treatments that are often harsh enough to result in significant coarsening of the Au particles. Residual S or P, in the form of stable sulfate and phosphate, could poison the Au particles when used as catalysts. Thus, there is a strong interest to identify alternate stabilizers that interact more weakly with Au and can be removed by oxidation more easily, such as ligands with amino

or carboxylate groups, since the strength of interaction follows the order (SH>P>N>O).

We have been exploring different approaches to synthesize nanosize metal particles.[38, 39] In one approach that was facilitated by amine and titanyl modified oligomeric hydrosiloxanes, Au nanoparticles between 1.75 and 2.25 nm and with very tight particle size distributions were obtained.[39] This method has an advantage in that oxidative removal of the organic groups attached to the siloxane oligomer would result in the metal particles dispersed in a mixed Ti-Si oxide. This is also a high yield process because all the added metal could be incorporated into the resulting colloid, a fact that could be important for noble metals. Thus, it appears that this is a promising approach that deserves further development and understanding for the synthesis of subnanometer Au particles.

We report here the results of using a modified version of this method by using only amine functionalized hydrosiloxane to successfully prepare subnanometer Au particles with narrow size distributions - a feat that has been known difficult to accomplish without using a strong stabilizer. In following the synthesis process with solution NMR and with use of model compounds, we gained important insights into the parameters that control Au particle sizes. We evaluated the requirement for proximal placement of the amine ligand and the reductant and established the importance of the steric hindrance offered by the oligomer. We collected evidence of binding of the amine ligand to the Au cation precursor and to the Au particles. Finally, we demonstrated that these Au nanoparticles are catalytically active.

B Experimental

B.1 Materials.

Poly(methylhydro)siloxanes (PMHS **I**) with trimethylsiloxy termination (1700-3200 g/mol average molecular weight, 12-45 cSt viscosity, average degree of oligomerization estimated by NMR spectroscopy 38 siloxane units), palladium hydroxide on carbon (20 wt.% loading), tetrahydrofuran (anhydrous, 99.9%), hexanes (95%), triethylsilane (99%), Au(III) chloride trihydrate (≥99.9% trace metals basis) and Au(III) chloride (≥99.99% trace metals basis) were purchased from Sigma-Aldrich. Celite 545 (filter aid, powder) and sodium sulfate (anhydrous, ≥99.0%) were from EMD Chemicals. Ethyl ether (anhydrous, ≥99.0%) was from Mallinckrodt Chemicals. Calcium sulfate ($CaSO_4$) (Drierite, without indicator, 20-40 mesh) was from Acros Organics. N-methyl-aza-2,2,4-trimethylsilacyclo-pentane was purchased from Gelest. All solvents (anhydrous), reagents and catalysts were used without further purification.

B.2 Synthesis of siloxanes oilgomers/compounds.

B.2.1 Oligomers based on PMHS: N-PMHS IV, N-SiH-PMHS V, and Me-SiH-PMHS VI. *N-PMHS **IV***: Synthesis of **IV** is shown in Scheme 1. 0.64 mL PMHS **I** possessing 10 mmol of SiH was added to 10 mL THF in a Schlenk flask. Excess H_2O (17 mmol) was used to completely oxidize SiH to silanols (SiOHs) in the presence of 30 mg Pearlman's catalyst (20 wt% $Pd(OH)_2/C$) to form **II**.[40] This reaction was followed by monitoring the hydrogen gas evolved. At the cessation of H_2 evolution, the reaction mixture was dried thoroughly using Na_2SO_4. The Pd catalyst was removed using column chromatography. The solution containing **II** was layered under N_2 flow onto a column composing of a layer of $CaSO_4$ sandwiched between layers of Celite using diethyl ether as the eluent.[39] The purified **II** was kept as a dilute solution to minimize self-condensation until use. The desired oligomer **IV** was formed by reacting the SiOH groups of **II** quantitatively with N-methyl-aza-2,2,4-trimethylsilacyclopentane in a Schlenk flask. The mixture was stirred for 20 min at room temperature followed by solvent removal at 50 mtorr pressure to generate **IV**, which was a viscous clear liquid. The ^1H, ^{13}C, ^{29}Si and HSQC NMR spectra of N-PMHS **IV** are shown in Figure S1; ^1H NMR (400 MHz, $CDCl_3$) δ 0.1-0.2 ((-Si(CH_3)$_3$, -Si(CH_3)$_2$, -SiCH_3); 0.38 (-SiCH_2); 0.63 (-SiCH_2); 0.80 (N*H*); 0.89 (CH_3CH-); 1.74 (CH_3C*H*-); overlapped 2.35 (-NHCH_2, -NHCH_3); 7.26 (CDCl3). ^{13}C NMR (100 MHz, $CDCl_3$) δ -2.65 (-Si(CH_3)$_3$); 1.07 (-SiCH_3); 1.34 (-Si(CH_3)$_2$); 20.90 (CH_3CH-)); 24.49 (-SiCH_2); 29.02 (CH_3C*H*-); 36.53 (-NHCH_3); 61.62 (-NHCH_2); 77.00 (CDCl3). ^{29}Si NMR (80MHz, $CDCl_3$) δ -67.90 (-*Si*CH_3); 6.99 (-*Si*(CH_3)$_3$); 8.49 (-*Si*(CH_3)$_2$).

*N-SiH-PMHS **V** and Me-SiH-PMHS* **VI**: Using the same procedure to form **II**, but with the added H_2O limited to 5 mmol**, III** was formed with only 50 % of SiH oxidized to the corresponding SiOH groups. After the SiOH groups in **III** was reacted quantitatively with N-methyl-aza-2,2,4-trimethyl-silacyclopentane, N-SiH-PMHS **V** was formed. **V** was characterized with NMR and the spectra were shown in Figures S-2. ^1H NMR (400 MHz, $CDCl_3$) δ 0-0.013 (-Si(CH_3)$_3$, -Si(CH_3)$_2$, -SiHCH_3, -SiCH_3);); 0.36(-SiCH_2); 0.61 (-SiCH_2); 0.82 (N*H*); 0.9 (CH_3CH-); 1.79 (CH_3C*H*-); overlapped 2.42 (-NHCH_2, -NHCH_3); 4.7 (Si-*H*); 7.26 (CDCl3).^{13}C NMR (100 MHz, CDCl3) δ -2.61 (-Si(CH_3)$_3$); 1.05 (-SiCH_3); 1.33 (-Si(CH_3)$_2$); 20.92(CH_3CH-)); 24.51 (-SiCH_2); 29.04 (CH_3C*H*-); 36.56 (-NHCH_3); 61.64 (-NHCH_2); 77.00 ($CDCl_3$). ^{29}Si NMR (80MHz, CDCl3) δ -66.82 (-*Si*CH_3); -36.51 (-*Si*HCH_3); 6.28 (-*Si*(CH_3)$_3$); 7. 90 (-*Si*(CH_3)$_2$).

III was reacted for 2 h with butyl(chloro)dimethylsilane in the presence of diethylamine as the chloride scavenger to form *Me-SiH-PMHS* **VI**. After the reaction, the white solid diethylamine hydrochloride was removed by filtration and **VI** was purified by vacuum evaporation to 50 mtorr. The clear viscous liquid **VI** was characterized using NMR (Figure S-3). ^1H NMR (400 MHz, $CDCl_3$) δ 0.12-0.37 (-Si(CH_3)$_3$, -Si(CH_3)$_2$, -SiHCH_3, -SiCH_3);); 0.48 (-SiCH_2); 0.84 (CH_3CH$_2$-); 1.17 (-SiCH$_2$CH_2CH$_2$); 1.60 (CH_3CH_2-); 5.01 (Si-*H*); 7.26 ($CDCl_3$). ^{13}C NMR (100 MHz, $CDCl_3$) δ -3.17 (-Si(CH_3)$_3$); -0.44 (-Si(CH_3)$_2$); 0.5 (-SiCH_3); 1.21 (-SiHCH_3); 13.34 (CH_3CH$_2$-); 17.37 (-SiCH_2); 24.95 (CH_3CH_2-); 25.95 (-SiCH$_2$CH_2CH$_2$); 77.00($CDCl_3$). ^{29}Si NMR (80MHz, $CDCl_3$) δ -66.47 (-*Si*CH_3); -34.85 (-*Si*HCH_3); 7.23 (-*Si*(CH_3)$_3$); 8.66 (-*Si*(CH_3)$_2$).

B.2.2 Trisiloxanes: $HSiMe_2OSiPh_2OSiMe_2C_4H_8NHCH_3$ VIII. Disiloxane $HSiMe_2OSiPh_2OH$ **VII** was prepared following the procedure described in ref.[41] by coupling

diphenylsilane diol with dimethylchlorsilane. **VII** (5 mmol) was dissolved in 10 mL dry THF in a Schlenk flask in a N_2 glove box. While stirring, 5 mmol N-methyl-aza-2,2,4-trimethylsilacyclopentane was added to react with the SiOH groups of **VII** quantitatively. The mixture was stirred for 20 min and the solvent was removed by evacuation to 50 mtorr to yield a viscous colorless liquid of the desired product **VIII**. NMR characterization are shown in Figure S4. ^{1}H NMR (400 MHz, $CDCl_3$) δ 0.12 (-Si(CH_3)$_2$CH$_2$); 0.19(-SiH(CH_3)$_2$); 0.44 (-SiCH_2); 0.71 (-SiCH_2); 0.90 (CH_3CH-); 1.77 (CH$_3$CH-); overlapped 2.33 (-NHCH_2, -NHCH_3); 4.84 (Si-H); 7.32-7.39 and 7.56-7.58 (-C$_6H_5$); 7.26 ($CDCl_3$). ^{13}C NMR (100 MHz, $CDCl_3$) δ 0.73 (-Si(CH_3)$_2$CH$_2$);1.34 (-SiH(CH_3)$_2$); 20.97(CH_3CH-)); 24.40 (-SiCH_2); 28.93 (CH$_3$CH-); 36.47 (-NHCH3); 61.52 (-NHCH_2); 127.6, 129.76,134.10,136.09 (-C$_6$H$_5$); 77.00 (CDCl3). ^{29}Si NMR (80MHz, $CDCl_3$) δ -46.03 (-Si(C$_6$H$_5$)$_2$); -4.76 (-SiH(CH$_3$)$_2$); 10.08 (-Si(CH$_3$)$_2$CH$_2$).

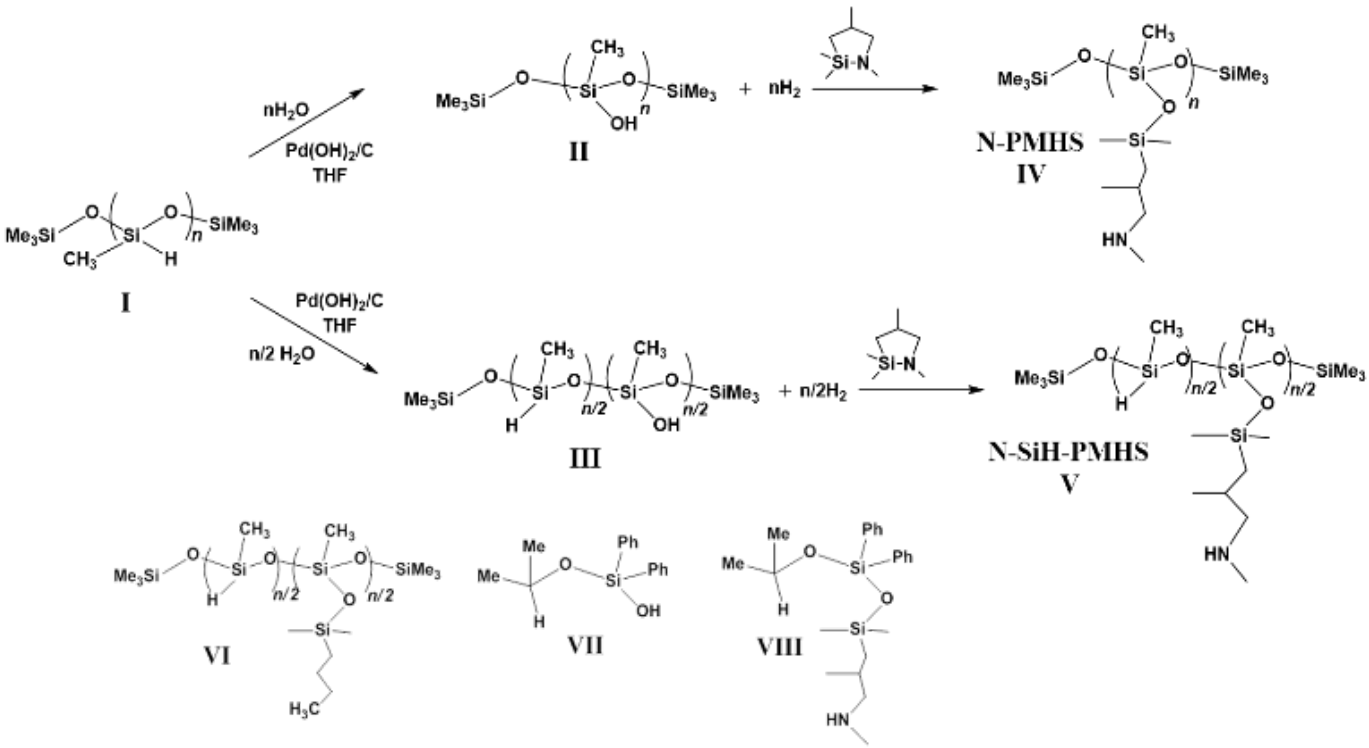

Scheme 1. Synthesis of N-PMHS **IV** and N-SiH-PMHS **V**, and structures of **VI**, **VII**, and **VIII**.

B.2.3 Synthesis of amine functionalized Au colloid. Chloro(tetrahydrothiophene)gold(I) (Au(THT)Cl) was synthesized similar to the work of Uson et al.[42] Aliquots of 6 mM Au(THT)Cl solution in THF in a N_2 filled Schlenk flask was added to ice-cooled vials containing either oligomer **IV**, **V**, or **VI**, or compound **VIII** in THF solution (Fig. 1). The amount of oligomer used was calculated to result in a functional group (amine or –Me2BuSi) to Au molar ratio of 10. When SiH reductant was not an integral part of the oligomer, triethylsilane diluted in THF was added as the reducing agent 1 h after mixing. Two different ratios 3:1 and 10:1 of SiH:Au were examined. Then THF was added to result in a total solution volume of 10 mL and a Au concentration of 3 mM. The mixture was stirred in an ice bath for another hour. Au/SiO_2 was prepared by depositing Au colloid solution in THF onto Cabosil-L90 and calcined in a stream of O_3 at 150 °C, similar to the work of Mashayekhi et al.[39]

B.3 Characterization.

^{1}H, ^{13}C and ^{29}Si NMR spectra were recorded with an Agilent DD2 spectrometer, operated at 400 MHz for ^{1}H, 100 MHz for ^{13}C, and 79 MHz for ^{29}Si. NMR spectra of the moisture sensitive

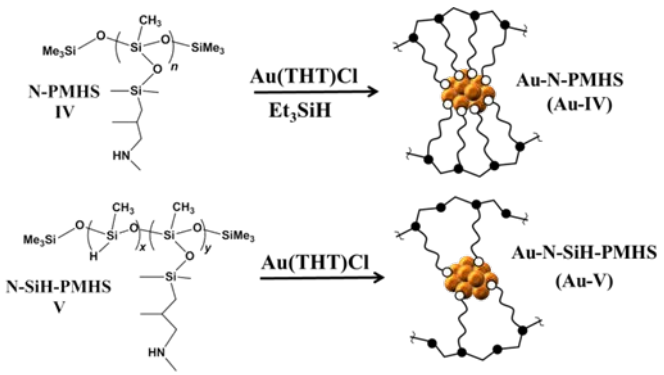

Fig. 1. Scheme for synthesis of amine-stabilized Au colloid. Filled black circles denote Si atoms, open circles denote amine functionality, and gold circles are Au atoms. For clarity, only a

section of two functionalized PMHS oligomers are shown (rearrange so it goes with the rest of fig.1).

compound were recorded in sealed J. Young NMR tubes. The ^{1}H and ^{13}C NMR chemical shifts, reported relative to $SiMe_4$, were determined by secondary references to the residual ^{1}H and ^{13}C peak of the deuterium solvent resonances. ^{29}Si NMR chemical shifts were referenced to TMS at 0.0 ppm. The chemical shifts reported are in ppm and coupling constants in Hz. All the NMR data were processed and analysed by MNova 9.0 software.

High angle annular dark field (HAADF) STEM images were obtained using a JEOL 2100-F transmission electron microscope with a field emission gun at 200 kV, which has a spatial resolution of 0.3 nm. Particle size analyses were performed using the program Image J. A Brookhaven BI9000 high speed correlator. Dynamic Light Scattering (DLS) instrument was used to measure the hydrodynamic diameters of the oligomer-coated Au nanoparticles. The incident light source was a 3 W Ar-ion laser operating at 514 nm. The sample concentration was 1 mg/mL and the cuvette volume was 300 µL. UV-vis absorption spectra of the Au colloid solutions were acquired using a HP (Agilent) 8452 diode array spectrophotometer. In a typical procedure, a freshly prepared Au colloid sample was diluted to 0.5 mM with cold THF and kept at ice temperature and away from light until analysis. The procedure was the same for aged samples that had been stored in the refrigerator at 3 mM concentration.

Small angle X-ray scattering and X-ray absorption measurements of 3 mM Au colloids in THF was measured at the 12-ID-B and 12-BM-B line of the Advanced Photon Source of Argonne National Laboratory. The SAXS data were fitted with Shulz-Zimmerman distribution function.

B.4 Catalytic reduction of *p*-nitrobenzaldehyde with triethylsilane.

Triethylsilane (0.05 mL, 0.3 mmol) was added to an ethanol suspension (1.5 mL) of *p*-nitrobenzaldehyde (43 mg, 0.28 mmol) and Au-N-SiH-PMHS (1.5 mL, 3 mM Au in THF). The resulting mixture was stirred in the dark under N_2 for 16 h, after which the solvent was evaporated and the products were analyzed by ^{1}H NMR after dissolving in $CDCl_3$. The resonances of the aldehyde group of the starting material (10.17 ppm) and the imine product (10.12 ppm) and the CH_2 signal of the alcohol product (4.84 ppm) were used for quantification.

C. Results and Discussion

C.1 Interaction of Au(THT)Cl with N-PMHS IV and N-SiH-PMHS V.

The interaction of Au(THT)Cl with the amino groups on N-PMHS **IV** and N-SiH-PMHS **V** were examined as a function of time using ^{1}H and ^{13}C NMR. Exposure of **IV** or **V** to Au(THT)Cl resulted in three sets of changes in the spectra (Figs. 2, 3, and S5): (1) Appearance of sharp resonances at δ 1.9 and 2.8 ppm due to unbound THT. (2) Changes in the resonance associated with the majority of the –N*H* protons (Fig. 2, highlighted by ovals) and the protons of N–CH_3 and N–CH_2– groups at ~δ 2.3-2.4 ppm (Fig. 2). (3) Appearance of a broad resonance at δ ~2.92 ppm (Fig. 3) assigned to the N–CH_3 of the amino groups of **IV** coordinated to Au(I), and at δ ~2.60 ppm assigned to the N–CH_2– of the same group. These changes will be discussed in the ensuing paragraphs. It should be noted that with an amine to Au ratio of 10 in these samples, direct observation of amine coordination to Au would be difficult because of its limited concentrations. The large excess of amine also implied that in the mixture of Au and N-SiH-PMHS**,** there was a large excess of -SiH groups to reduce Au(I) to Au(0). This contrasted with the mixture of Au and N-PMHS where there was ~1 residual –SiH to 60 –RNH in the oligomer, which was equivalent to 1 –SiH to 6Au (determined from NMR peak area of Si–*H*).

C.1.1. δ 1.9 and 2.8 ppm resonances. After mixing Au(THT)Cl and N-PMHS **IV** or N-SiH-PMHS **V**, the appearance of resonances at δ 1.9 and 2.8 ppm in the ^{1}H NMR due to unbound THT and the disappearance of the broad resonances of bound THT (δ 1.9-2.4 and 3.1-3.6 ppm) were indicative of displacement THT originally coordinated to Au (Fig. S-5). A similar displacement of the THT ligand from Au(I) was also observed in a control experiment in which diethylamine (Et_2NH) was used instead of N-PMHS (Fig. S-6). These observations were consistent with Eq. 1 and with previous reported literature.[43] Using an added standard for quantification, it was determined that the displacement of THT was complete within 1 h for both Au-**IV** and Au-**V**. The strength of the interaction of amine with AuCl was purported to derive from hydrogen bonding between N–H and Cl and aurophilic interactions.[44]

–NHR + Au(THT)Cl = THT + Au(NHR)Cl (1)

C.1.2. –NH, N–CH_3 and N–CH_2– protons. The resonances of these protons are shown in Fig. 2. The two protons of the N–CH_2– are diastereotopic and appeared as the broad multiplet at the same general position as the N–CH_3 resonance (~δ 2.3-2.4 ppm, right panel). Within ±20%, the integrated areas of –NH, N–CH_2– and N–CH_3 accounted for all, or at least a large majority, of the protons associated with the amines in the samples.

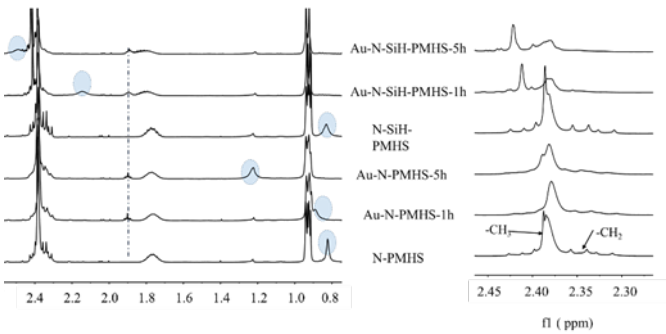

Fig. 2. ^{1}H NMR of various sample after addition of Au(THT)Cl to N-PMHS **IV** or SiH-N-PMHS **V** after 1 or 5 h. (Left) Region of spectra that showed resonances of unbound THT (marked by

dotted line), NH (blue ovals), and CH_3+CH_2 at δ ~2.3 to ~2.4 ppm. (Right) Expanded view of the resonances at δ~2.3 to ~2.4 ppm.

The presence of SiH in **V** caused rapid reduction of Au(I) after mixing and large changes in the resonances of –N*H*, and N–C*H*$_2$– and N–C*H*$_3$ (Fig. 2). The–N*H* resonance was shifted from δ 0.8 to 2.1-2.4 ppm. The overlapping N–C*H*$_2$– and N–C*H*$_3$ peaks now appeared as two peaks, a broader one at δ ~2.38 ppm and a narrower one at δ ~2.42-3.43 ppm. These extensive spectroscopic changes indicated structural changes in the oligomer. We hypothesized that the reduction of Au(I) by silane resulted in the formation of –SiCl (Eq. 2). The formed –SiCl could readily react with a nearby free –RNH in the manner shown in Eq. 3[45] to form a new silazane bond and the concomitant protonation of another amine. These structural modifications caused conformational changes of the oligomer and the observed spectroscopic changes.

$$2NHRAu^{I}Cl+2R_3SiH=2NHRAu^{0}+2R_3SiCl+H_2 \quad (2)$$

$$R_3SiCl+2NHR_2 = R_3Si\text{-}NR_2+R_2NH_2^{+}Cl^{-} \quad (3)$$

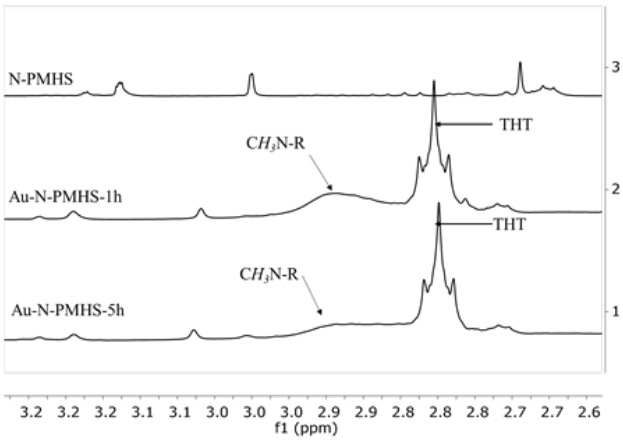

Fig. 3. ^{1}H NMR of N-PMHS **IV** and Au-**IV**.

C.1.3. δ ~2.92 and ~2.60 ppm resonances. The third spectroscopic change after mixing Au(THT)Cl with **IV** was the appearance of a new broad resonance at δ ~2.90 ppm (Fig. 3). This new resonance was observable only for this Au-**IV** mixture and not for the Au-**V** mixture, or in samples without Au. Thus, it was due to the interaction of Au(I) with **IV**. We assigned this peak to the protons of N–C*H*$_3$ that was directly ligated to Au(I)Cl. The assignment was supported by HSQC data (Fig. S-8).

The assignment of the very broad, low intensity peak around δ 2.60 ppm to N–C*H*$_2$– of the amine ligated to Au(I) was also based on HSQC results, but was less definitive due to the low intensities of the resonance peaks consequent of the protons being diastereotopic and being split by multiple neighboring protons (Fig.S-8). Nonetheless, the assignment was supported by the fact this correlation in HSQC was more obvious when the Au concentration was increased to an amine/Au ratio of 2.5 (Fig. S-9).

The ratio of ligated amine to Au was 1.6 and 1 for the mixture of **IV** and Au(THT)Cl when the amine/Au ratios were 10 and 2.5, respectively. In contrast, the ratio was 2 using the model compound Et_2NH. This lower ratio for Au-**IV** could be due to the fact that in **IV**, there might not be two amino groups in the same vicinity and the right configuration to coordinate to Au(I) simultaneously.

Addition of the reductant Et_3SiH to the solution of **IV** bound to Au(I) (amine/Au=2.5) caused the δ 2.90 ppm peak to disappear within 10 min (Fig. S-10), thus further confirming that this peak was associated with amines coordinated to Au(I). This was also in line with the observation that this peak decreased in intensity 5 h after mixing Au(THT)Cl and **IV**, which could be explained by the small amount of residual SiH groups in **IV**, and its absence in the Au-**V** samples that had little unreduced Au.

C.2 Determination of particle size and stability of Au colloidal particles.

The importance of the role of oligomer and the proximity of ligating amine and silane reductant on the Au particle size was examined by using four different combination of silane reductant and amine ligands:

1) amine and silane on the same oligomer (N-SiH-PMHS **V**)
2) amine on oligomer and silane added independently (Et_3SiH + N-PMHS **IV**).
3) oligomer possessing silane but no amine (Me-SiH-PMHS **VI**).
4) trisiloxane molecule containing both silane and amine ($HSiMe_2OSiPh_2OSiMe_2C_4H_8NHCH_3$ **VIII**).

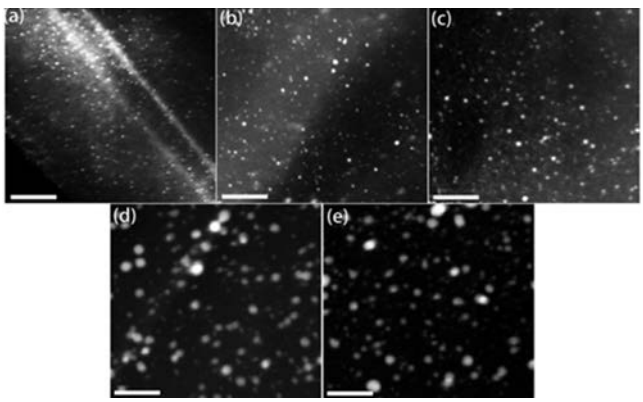

Fig. 4. STEM images of the Au colloid, (a)-(e) corresponded to experiments 1 to 5 in Table 1, respectively. Scale bar is 20 nm.

In all these experiments, the Au/amine ratio was kept the same at 10. Additional experiments were conducted to examine the effect of preparation temperature and Au/SiH ratio. Table 1 shows the result of these experiments where the average Au particle sizes were determined from STEM and representative STEM images are shown in Figure 4. Not shown in the Table is

the preparation using an oligomer without amine ligand (Me-SiH-PMHS **VI**) which produced large nonuniform Au agglomerates >10 nm (STEM image Fig. S-11). Thus, not surprisingly, stabilization by amine ligands is essential for the formation of small Au particles.

A comparison of sample **a**, prepared using N-SiH-PMHS **V** with both silane and amine present in the oligomer, and sample **c**, prepared with N-PMHS **IV** that did not possess silane, showed that both the Au particle size and size distribution (Table 1) were smaller for synthesis mediated with **V.** The contribution of the proximity of silane and amine to these differences may be minor as our NMR results established that Au(I) was bound to the amine upon mixing of Au(THT)Cl and **IV.** Thus, when Au(I) was reduced by the externally added silane, a high concentration of amines was in the proximity of Au, and the environment would be similar to the reduction of Au using **V.** On the other hand, the two synthesis were conducted with different concentrations of oligomers in order to maintain an identical concentration of amine. Since **V** had half the amount of amine as **IV**, its concentration was twice as high. Thus, the Au density per oligomer **V** was half of that per oligomer **IV**. The lower Au density would result in a thicker layer of the viscous siloxane surrounding every Au particle, which should be more effective in retarding agglomeration by inter-oligomer diffusion of Au particles.

The importance of steric barrier rather than the proximity of the reducing and ligating functionalities in controlling the Au particle size was further underscored by the large and highly non-uniform Au particles present in sample **d.** This preparation was conducted under identical conditions as sample **a**, except that a small molecule disiloxane **VIII** was used. Although **VIII** also possessed both SiH and amine functionalities, it was much less effective in providing steric barrier than the long flexible oligomer **V** in deterring Au particle agglomeration.

When the silane Et_3SiH was added externally, the preparation using a lower concentration of reductant resulted in smaller Au particles (compare samples **b** and **c**). Possibly, this was because the rate of reduction was slower at a lower reductant concentration, allowing more effectively amine coordination before Au agglomeration could take place. That the rate of reduction was important was consistent with the experiments to examine the effect of preparation temperature. With all other synthesis parameters identical, the Au particles prepared at ice temperature were smaller and more uniform than those prepared at room temperature (compare samples **b** and e). At a higher temperature, both the reduction rate and mobility of Au were expected to be higher, which would lead to larger Au particles.

Table 1. Average Au particle size in different preparations.

	Amine and silane carrier	Synthesis solution conditions[a]				Au colloid diameter (nm)	Au/SiO_2 diameter[f] (nm)
		[Olig][b] or [trisiloxane] mM	[amine][c] mM	Au/SiH	T (°C)		
a	N-SiH-PMHS **V**	1.6	30	1:10	0	0.69±0.13[d]	0.92±0.70[d]
b	Et_3SiH + N-PMHS **IV**	0.8	30	1:3	0	0.89±0.24[d]	1.95±0.67[d]
c	Et_3SiH + N-PMHS **IV**	0.8	30	1:10	0	0.94±0.32[d]	1.87±0.72[d]
d	Trisiloxane **VIII**	30[g]	30	1:10	0	3.05±2.51[e]	4.03±3.09[e]
e	Et_3SiH + N-PMHS **IV**	0.8	30	1:3	25	2.55±1.94[e]	2.99±1.89[e]

[a] N/Au atomic ratio was 10.
[b] Based on an average of 38 siloxane units per oligomer.
[c] Calculated using the extent of conversion of SiH to amino units and assuming an average of 38 siloxane units per oligomer.
[d] Based on 200 particles.
[e] Based on 500 particle.
[f] After deposition of colloidal particles onto SiO_2 and thermal treatment in an O_3 atmosphere at 150 °C.

In addition to STEM, other techniques were also used to characterize the Au-siloxane colloidal complexes. Dynamic light scattering (DLS), which provides information about the hydrodynamic diameters of colloidal particles, showed that the mean sizes of the colloidal particles were 1.5, 2.0, 2.7, and 5.6 nm, respectively for samples **a-d** (Fig. S-12), consistent with the trend found with STEM. Since the DLS data reflected the size of the colloid particles, that is, Au particles embedded in a

shell of organosiloxane oligomers, the particle sizes determined by this method was expected to be slightly larger than the Au particle size derived from the STEM data. For similar reasons, SAXS characterization of sample **a** (Fig. S-13) also showed much larger particles than those derived from STEM. XANES spectra of all these samples confirmed that all the Au were metallic (Fig. S-15).

Since the intensity of the DLS signal is proportional to (diameter)^6, the very narrow size distribution shown in the data indicated sample uniformity - a testimony that the method reported here was indeed facile and versatile, as no purification or separation step was employed after mixing the Au precursor and the oligomer.

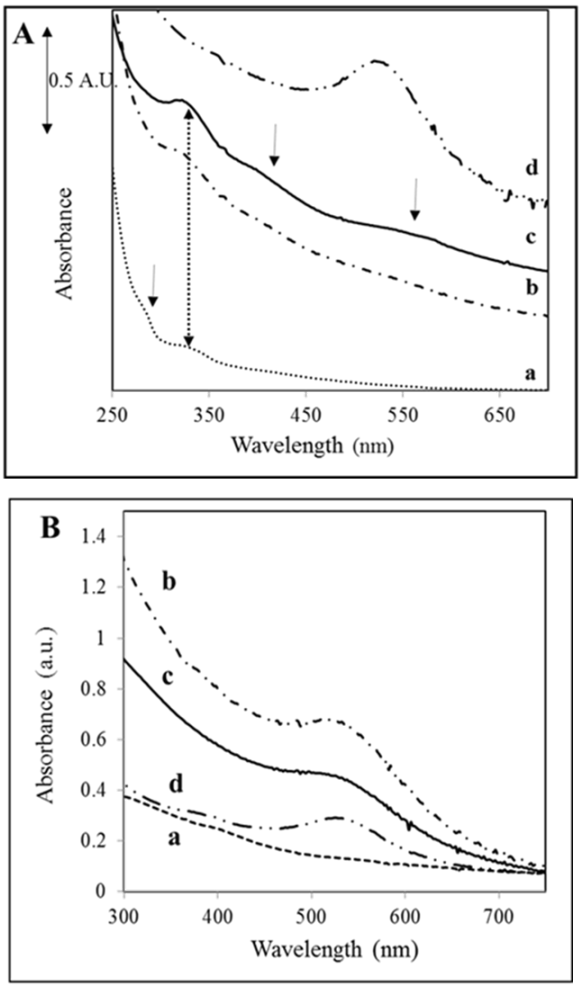

Figure 5. UV-visible spectra of samples **a-d** listed in Table 1. Panel A: Spectra taken 2 h after completion of synthesis and panel B: 4 weeks later. The spectra for samples **b-d**in panel A were displaced vertically from the baseline by 0.25 absorbance unit for clarity. HPLC grade THF was the solvent for samples. **a-c** in panel A, whereas Research grade was used for sample **d**. The concentrations of Au were the same for all samples.

UV-visible spectroscopy was also used to characterize the Au colloids. As shown in panel A of Figure 5, only sample **d** showed the characteristic surface plasmon resonance at 525 nm for Au nanoparticles > 2nm.[1] Spectra of all other samples showed only weak features: small peaks at 330 and 280 nm for sample **a**. , the barely detectable absorption at ~560 and ~410 nm, and more intense absorption at 330 nm for sample **b**. For sample **c** the absorptions at 560, 410, and 330 became easily identifiable.

The small absorption features detected for samples **a-c** suggested the presence of significant concentrations of some well-defined species. It has been shown by matrix isolation that atomic to trimeric Au showed electronic transitions within 200-400 nm due to transitions between discrete HOMO-LUMO levels.[46] For Au clusters encapsulated in well-defined poly(amidoamine) dendrimers, Zheng et al.[47] reported that the maxima of the excitation spectra for Au_5, Au_8 and Au_{13} clusters were 332, 385 and 431 nm, respectively. Negishi et al. found that the absorbance maximum of their glutathione capped clusters ranged from 330 nm to 570 nm for clusters with Au core sizes that ranged from 10-22.[48] Thus literature results suggested that these absorption features corresponded to very small Au clusters (<1 nm) It is likely that many of these clusters were too small to be observed with the STEM instrument we used (limit ~0.6±0.2 nm). Thus, in samples where UV-vis data suggested their presence, the average particle size of these samples should be smaller than those shown in Table 1. The variation of the density of these smaller particles were consistent with the trends determined by STEM.

These colloidal particles were quite stable on storage in the absence of light in a refrigerator. Nonetheless there was evidence of agglomeration with time. As shown in Figure 5 panel B, after 4 weeks of storage, with the exception of sample **a** the other samples all developed the plasmon peak around 520 nm that was characteristic of Au nanoparticles. Even the originally colorless solution of sample **a** turned brown, suggesting some degree of agglomeration. Since the Au particles in these samples were surrounded by siloxane oligomers, the initial growth of Au clusters probably occurred within the same Au-PMHS colloidal particle. With time, collisions between colloidal particles occurred where interparticle exchanges of Au particles took place that enabled their subsequent agglomeration.

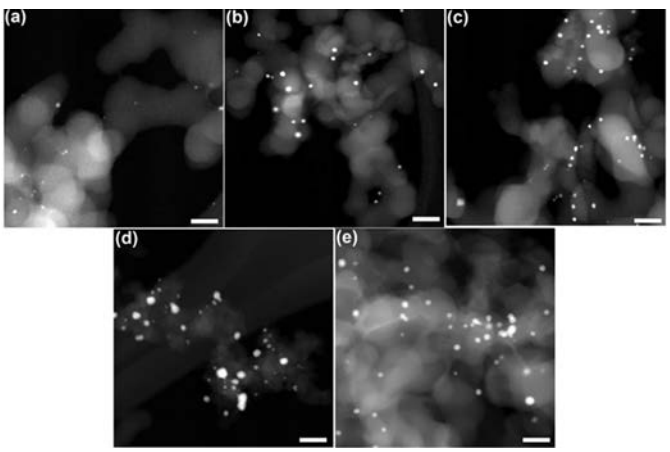

Fig. 6. STEM images of Au/SiO_2; images (**a**)-(**e**) corresponded to samples in Table 1 (last column). Scale bar is 20 nm.

Another measure of stability was to examine the degree of particle agglomeration after thermal treatment. We deposited these colloidal particles onto silica and thermally treated them in an O_3 atmosphere at 150ºC to remove all the organics and convert the siloxane into SiO_2. Particle growth occurred, but the Au particle sizes and uniformity for the different samples maintained the same trend as was observed for the parent colloidal samples (Table 1 and Fig. 6). The average Au particle size of sample **a** remained subnanometer.

C.3 Accessibility of Au colloids surface.

Sample **a** was chosen to test for catalytic activity to see whether Au clusters embedded in the oligomer was accessible to reactants. The test reaction was *p*-nitrobenzaldehyde reduction by triethylsilane (Et_3SiH) using equimolar quantities of the two reactants (Scheme 2). In this reaction, the product **IX** was formed by first reduction of *p*-nitrobenzaldehyde to *p*-aminobenzaldehyde, followed by the subsequent domino reaction of *p*-aminobenzaldehyde coupling with the nitrobenzaldehyde to form an imine bond. At the end of reaction, there were ~20% compound **IX** and ~8% *p*-nitrobenzyl alcohol in the product. Since the formation of each molecule **IX** consumes six silanes, the result indicated complete consumption of silane. In the absence of the Au colloid from Expt. 1, the yield of **IX** and *p*-nitrobenzyl alcohol were only 2% and 5%, respectively. Thus, the Au colloid was an active catalyst, and the Au particles were accessible for reaction.

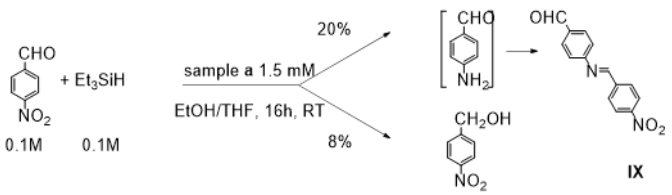

Scheme 2. Catalytic conversion of p-nitrobenzaldehyde catalysed by sample **a.**

Conclusions

Using the preparation of Au particles, we demonstrated a practical, convenient and facile method that does not rely on strong stabilizers to prepare metal colloids. The synthesis is mediated by siloxane oligomers containing both reducing (SiH) and ligating (amine) functionalities and permits controlled variation of metal particle size at subnanometer scale. Variation of the ratios of these functionalities and using small model molecules allowed us to identify relevant synthesis parameters, such as the extent of steric and ligand stabilization and the rates of reduction, that affect the properties of the resultant Au particles. Monitoring the synthesis with NMR at different stages of the synthesis showed the ready displacement of THT from Au by amines in the oligomer with the concomitant appearance of new NMR peaks associated with amines bound to Au(I). These peaks subsequently disappeared with the reduction to metallic Au.

The Au particles obtained by this method were quite stable, even after oxidation treatment to remove the organics. Since the principles used here are general, this method should be applicable to the synthesis of subnanometer particles of other supported late transition metals. Thus, it could have many potential applications when such particles are called for, such as in sensors and catalysis.

Acknowledgements

This work was supported by the Department of Energy, Basic Energy Sciences, grant no. DE-FG02-01ER15184. Z.W. and X.H. acknowledge funding support from China Scholarship Council. This work made use of the TEM and NMR in the EPIC facility of NUANCE Center and IMSERC facility at Northwestern University. This research used resources of the Advanced Photon Source, a U.S. Department of Energy (DOE) Office of Science User Facility operated for the DOE Office of Science by Argonne National Laboratory under Contract No. DE-AC02-06CH11357

Notes and references

[a] Chemical and Biological Engineering Department, Northwestern University, Evanston, IL 60208, USA.
[b] School of Materials Science and Engineering, Northwestern Polytechnical University, Xi'an, Shaansi 710072, P. R. China
[c] X-ray Science Division, Argonne National Laboratory, Argonne, IL 60439, USA
[d] Chemistry Department, Northwestern University, Evanston, IL 60208,USA.
*Corresponding authors: m-kung@northwestern.edu and hkung@northwestern.edu

Electronic Supplementary Information (ESI) available: NMR, TEM, DLS, XANES, SAX and absorption wavelengths of Au clusters calculation based on Jellium model.

1. M. M. Alvarez, J. T. Khoury, T. G. Schaaff, M. N. Shafigullin, I. Vezmar and R. L. Whetten, *J. Phys. Chem. B*, 1997, **101**, 3706-3712.
2. J. F. Hicks, A. C. Templeton, S. Chen, K. M. Sheran, R. Jasti, R. W. Murray, J. Debord, T. G. Schaaff and R. L. Whetten, *Anal. Chem.*, 1999, **71**, 3703-3711.
3. R. Jin, *Nanoscale*, 2010, **2**, 343-362.
4. Y. Negishi, K. Nobusada and T. Tsukuda, *J. Amer. Chem. Soc.*, 2005, **127**, 5261-5270.
5. M. Zhu, C. M. Aikens, F. J. Hollander, G. C. Schatz and R. Jin, *J. Amer. Chem. Soc.*, 2008, **130**, 5883-5885.
6. M.-C. Daniel and D. Astruc, *Chem. Rev.*, 2004, **104**, 293-346.
7. J. Zheng, C. Zhang and R. M. Dickson, *Phys. Rev. Lett.*, 2004, **93**, 077402.
8. M. Haruta, *Gold Bull.*, 2004, **37**, 27-36.
9. J. Huang, T. Akita, J. Faye, T. Fujitani, T. Takei and M. Haruta, *Angew. Chem. Int. Ed.*, 2009, **48**, 7862-7866.
10. J. K. Edwards, B. Solsona, E. Ntainjua, A. F. Carley, A. A. Herzing, C. J. Kiely and G. J. Hutchings, *Science*, 2009, **323**, 1037-1041.
11. M. Turner, V. B. Golovko, O. P. Vaughan, P. Abdulkin, A. Berenguer-Murcia, M. S. Tikhov, B. F. Johnson and R. M. Lambert, *Nature*, 2008, **454**, 981-983.
12. M. Boronat, A. Leyva-Perez and A. Corma, *Acc. Chem. Res.*, 2014, **47**, 834-844.

13. A. Corma, P. Concepcion, M. Boronat, M. J. Sabater, J. Navas, M. J. Yacaman, E. Larios, A. Posadas, M. A. Lopez-Quintela, D. Buceta, E. Mendoza, G. Guilera and A. Mayoral, *Nature Chem.*, 2013, **5**, 775-781.
14. M. Flytzani-Stephanopoulos, *Acc. Chem. Res.*, 2014, **47**, 783-792.
15. W. Jiang, B. Y. Kim, J. T. Rutka and W. C. Chan, *Nature Nanotech.*, 2008, **3**, 145-150.
16. C. K. Kim, P. Ghosh, C. Pagliuca, Z.-J. Zhu, S. Menichetti and V. M. Rotello, *J. Amer. Chem. Soc.*, 2009, **131**, 1360-1361.
17. A. Verma, O. Uzun, Y. Hu, Y. Hu, H.-S. Han, N. Watson, S. Chen, D. J. Irvine and F. Stellacci, *Nature Mater.*, 2008, **7**, 588-595.
18. P. Zhao, N. Li and D. Astruc, *Coord. Chem. Rev.*, 2013, **257**, 638-665.
19. P. C. Ohara, D. V. Leff, J. R. Heath and W. M. Gelbart, *Phys. Rev. Lett.* , 1995, **75**, 3466-3469.
20. R. H. Terrill, T. A. Postlethwaite, C.-h. Chen, C.-D. Poon, A. Terzis, A. Chen, J. E. Hutchison, M. R. Clark and G. Wignall, *J. Amer. Chem. Soc.*, 1995, **117**, 12537–12548.
21. M. M. Alvarez, J. T. Khoury, T. G. Schaaff, M. Shafigullin, I. Vezmar and R. L. Whetten, *Chem. Phys. Lett.*, 1997, **266**, 91-98.
22. R. L. Whetten, J. T. Khoury, M. M. Alvarez, S. Murthy, I. Vezmar, Z. L. Wang, P. W. Stephens, C. L. Cleveland, W. D. Luedtke and U. Landman, *Adv. Mater.* , 1996, **8 (5)**, 428-433.
23. M. Brust, M. Walker, D. Bethell, D. J. Schiffrin and R. Whyman, *J. Chem. Soc., Chem. Commun.*, 1994, 801-802.
24. W. W. Weare, S. M. Reed, M. G. Warner and J. E. Hutchison, *J. Amer. Chem. Soc.*, 2000, **122(51)**, 12890–12891.
25. N. de Silva, J.-M. Ha, A. Solovyov, M. M. Nigra, I. Ogino, S. W. Yeh, K. A. Durkin and A. Katz, *Nature Chem.*, 2010, **2**, 1062-1068.
26. A. G. Kanaras, F. S. Kamounah, K. Schaumburg, C. J. Kiely and M. Brust, *Chem. Comm.*, 2002, 2294–2295.
27. J. M. Abad, I. E. Sendroiu, M. Gass, A. Bleloch, A. J. Mills and D. J. Schiffrin, *J. Amer. Chem. Soc.*, 2007, **129**, 12932-12933.
28. V. I. Pârvulescu, V. Pârvulescu, U. Endruschat, G. Filoti, F. E. Wagner, C. Christian Kübel and R. Richards, *Chem. Europ. J.*, 2006, **12(8)**, 2343-2357.
29. Y. Negishi and T. Tsukuda, *J. Amer. Chem. Soc.*, 2003, **125**, 4046-4047.
30. M.-Y. Tsai and J.-C. Lin, *J. Biomed. Mater. Res.*, 2001, **55**, 554-565.
31. F. Zhang, Y. Zhou, Y. Chen, Z. Shi, Y. Tang and T. Lu, *J. Coll. Interface Sci.*, 2010, **351(2)**, 421-426.
32. D. Wang, Y. Liu, X. Zhou, J. Sun and T. You, *Chem. Lett.*, 2007, **36 (7)**, 924-925.
33. P. D. Jadzinsky, G. Calero, C. J. Ackerson, D. A. Bushnell and R. D. Kornberg, *Science*, 2007, **318**, 430-433.
34. M. W. Heaven, A. Dass, P. S. White, K. M. Holt and R. W. Murray, *J. Amer. Chem. Soc.*, 2008, **130**, 3754-3755.
35. M. Zhu, E. Lanni, N. Garg, M. E. Bier and R. Jin, *J. Amer. Chem. Soc.*, 2008, **130**, 1138-1139.
36. J. F. Parker, J. E. Weaver, F. McCallum, C. A. Fields-Zinna and R. W. Murray, *Langmuir*, 2010, **26**, 13650-13654.
37. M. N. Martin, D. Li, A. Dass and S. K. Eah, *Nanoscale*, 2012, **4**, 4091-4094.
38. B. Fu, M. N. Missaghi, C. M. Downing, M. C. Kung, H. H. Kung and G. Xiao, *Chem. Mater.*, 2010, **22**, 2181-2183.
39. N. A. Mashayekhi, Y. Y. Wu, M. C. Kung and H. H. Kung, *Chem. Commun.*, 2012, **48**, 10096-10098.
40. Y. Li and Y. Kawakami, *Macromolec.*, 1999, **32**, 3540-3542.
41. W. Xue, M. C. Kung and H. H. Kung, *Chem. Commun.*, 2005, 2164-2166.
42. R. Uson, A. Laguna and M. Laguna, *Inorg. Syn.*, 1989, **26**, 85-91.
43. S. Gomez, K. Philippot, V. Colliere, B. Chaudret, F. Senocq and P. Lecante, *Chem. Commun.*, 2000, 1945-1946.
44. B. Ahrens, P. G. Jones and A. K. Fischer, *Eur. J. Inorg. Chem.*, 1999, 1103-1110.
45. H. Yoshida, T. Morishita, H. Fukushima, J. Ohshita and A. Kunai, *Org. Lett.*, 2007, **9**, 3367-3370.
46. W. Harbich, S. Fedrigo, J. Buttet and D. M. Lindsay, *J. Chem. Phys.*, 1992, **96**, 8104-8108.
47. J. Zheng, C. Zhang and R. M. Dickson, *Phys. Rev. Lett.*, 2004, **93**, 077402/077401-077402/077404.

Graphical Abstract
54